CO_2 dissociation activated through electron attachment on the reduced rutile TiO_2(110)-1×1 surface

Shijing Tan, Yan Zhao, Jin Zhao, Zhuo Wang, Chuanxu Ma, Aidi Zhao, Bing Wang,* Yi Luo, Jinlong Yang, and Jianguo Hou†

Hefei National Laboratory for Physical Sciences at the Microscale, University of Science and Technology of China, Hefei, Anhui 230026, P. R. China

(Received 31 August 2011; published 13 October 2011)

Converting CO_2 to useful compounds through the solar photocatalytic reduction has been one of the most promising strategies for artificial carbon recycling. The highly relevant photocatalytic substrate for CO_2 conversion could be the popular TiO_2 surfaces. However, the lack of accurate measurements for the energy level alignment that determines the CO_2 reduction on TiO_2 has limited our ability to control these complicated photocatalysis processes. We report here a systematic study on the reduction of CO_2 at specific sites of the rutile TiO_2(110)-1 × 1 surface using scanning tunneling microscopy at 80 K. The dissociation of CO_2 molecules is found to be activated by one electron attachment process with an energy threshold of 1.8 eV above the Fermi level (or 1.4 eV above the TiO_2 conduction band onset), while the lowest unoccupied molecular orbital (LUMO) of the adsorbed CO_2 is located at 2.3 eV with respect to the Fermi level. The observed dependence of the dissociation rate on the tunneling current suggests that the reduction of CO_2 induced by the electron attachment is a single electron process. These practical information can be used to guide the design of effective catalysts for CO_2 photoreduction.

DOI: 10.1103/PhysRevB.84.155418 PACS number(s): 34.80.Ht, 31.70.−f, 68.37.Ef, 68.43.Rs

I. INTRODUCTION

During the last decades, there is a growing research interest in converting CO_2 into value added products for energy production to actively reduce the CO_2 emission.[1–8] One of the promising strategies is to convert CO_2 into CO or hydrocarbons by photoreduction,[9–13] although its efficiency still needs to be significantly improved.[14] The decisive step in the CO_2 reduction is to effectively generate $CO_2^{\bullet-}$, the electron attached state of CO_2,[15,16] which is controlled by the reduction potential of the $CO_2^{\bullet-}/CO_2$ redox couple. The search for a good match between the reduction potential and the conduction band (CB) of the photocatalytic substrates has been the central focus of many studies. It is found that even for the widely used photocatalyst, TiO_2, a strong mismatch occurs,[3,5,16–19] resulting in highly unfavorable electron transfer from the photoexcited conduction band of the TiO_2 to the adsorbed CO_2 molecules. Such an energy mismatch could be compensated by either introducing additional catalysts to assist the electron transfer or modifying the conduction band of the photocatalyst with chemical modifications.[5] However, the optimization procedures are hampered by the lack of accurate data for the bonding sites of CO_2 on the substrates and the energy position of the reduction potential. In this case, an atomistic study with scanning tunneling microscopy (STM) is highly desirable since it can not only provide a complete picture for the specific adsorption sites of single CO_2 molecules, but also determine the reduction potential through the detection of the unoccupied molecular orbitals. Here, we present a comprehensive study on STM induced one-step direct reduction process of CO_2 to CO on reduced rutile TiO_2(110)-1 × 1 surface at 80 K. The adsorption sites of CO_2 at various coverages, the reduction potential of the $CO_2^{\bullet-}/CO_2$ redox couple and the reaction rate are accurately determined. The underlying mechanisms are fully examined with the help of first-principles calculations.

II. EXPERIMENTAL AND CALCULATION METHOD

Our STM experiments were conducted with a low-temperature scanning tunneling microscope (Matrix, Omicron) in an ultrahigh vacuum system with a base pressure less than 3×10^{-11} Torr, which has been baked out sufficiently for a long time to minimize the background water in the chamber. The STM measurements were mainly performed at 80 K. An electrochemically etched polycrystalline tungsten tip was used in STM experiments. The rutile TiO_2 (110) sample (Princeton Scientific Corporation) was prepared by repeated cycles of ion sputtering (3000 eV Ar^+) and annealing (at 900 K). The CO_2 gas (purity of 99.999%) was used.

A TiO_2 (110)-1 × 1 surface was modeled by periodically repeated slabs consisting of a (6 × 2) cell with 5 O-Ti-O layers separated by 10 Å of vacuum. All the calculations are performed with the Vienna *ab initio* simulation package (VASP) with the generalized gradient approximation of Perdew, Burke, and Ernzerhof (PBE-GGA).[20] A plane-wave basis set with energy cutoff of 400 eV and the projector augmented wave (PAW) potential was employed.[21] Monhkorst-3 Pack grids of (2 × 2 × 1) k points were used for the (6 × 2) unit cells. Since the CO_2 molecule is adsorbed on only one side of the slab, dipole correction is included in the calculations. During the optimization, atoms were allowed to relax in the upper three layers and all the structures are relaxed until self-consistent forces are smaller than 0.02 eV/Å.

III. RESULTS AND DISCUSSION

Our first task is to determine the adsorption site of CO_2 molecules. Figure 1 shows the STM images within the same area of hydroxyl-free TiO_2(110)-1 × 1 surface before and after the exposure of 3.0 Langmuir CO_2 (1 Langmuir = 1×10^{-6} Torr s) at 80 K. After the CO_2 exposure, it is observed that the CO_2 molecules only appear at the bridge-bonded oxygen

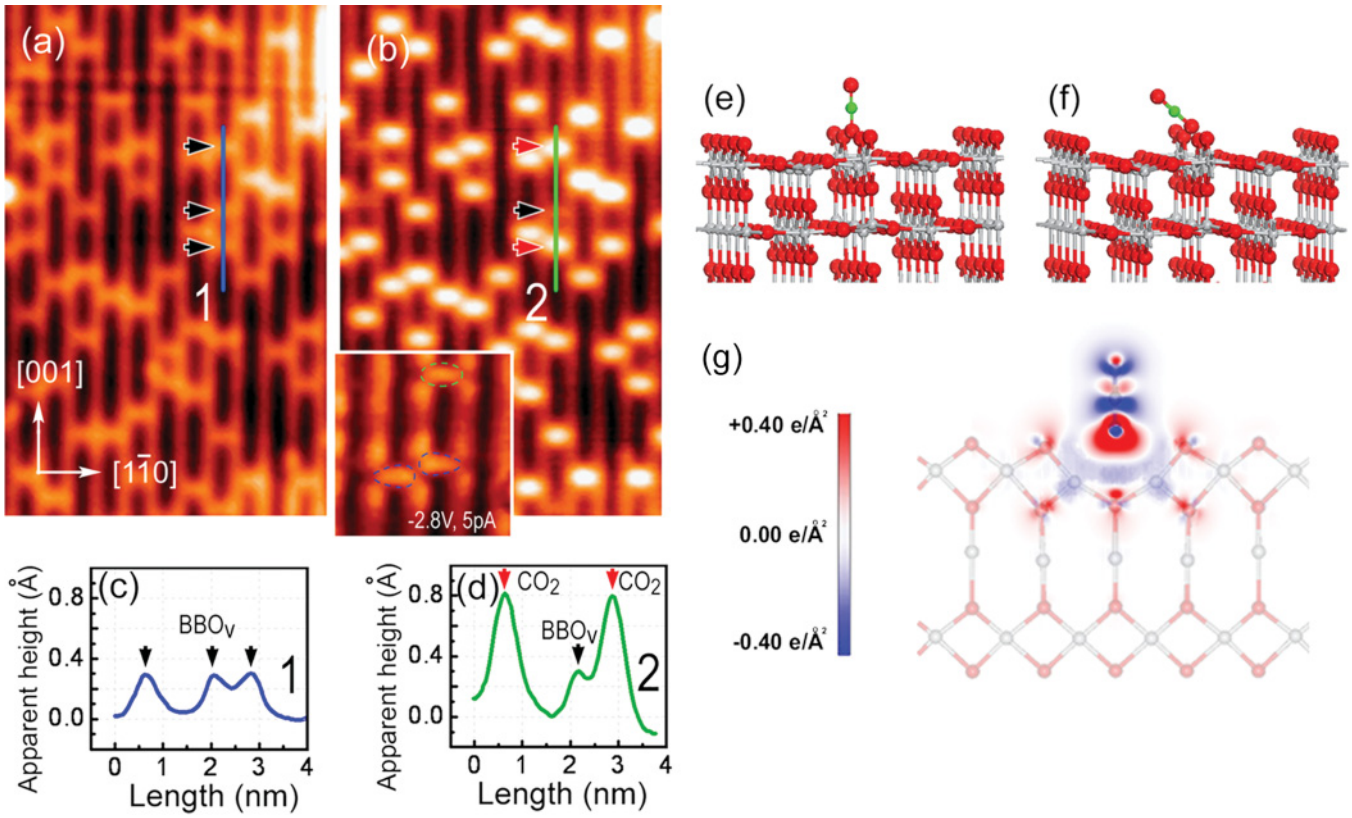

FIG. 1. (Color online) (a) and (b) Images of TiO_2(110)-1 × 1 before and after *in situ* CO_2 adsorption at 80 K. (Size: 7.2 × 11.4 nm^2, imaging conditions: 1.0 V, 10 pA.) (c) and (d) Line profiles showing the apparent height of adsorbed CO_2 in comparison with the BBO_V. The inset in (b) shows the occupied-state (−2.8 V) image of adsorbed CO_2 on TiO_2 (2.0 × 2.0 nm^2), showing coexistence of symmetric and asymmetric shapes of adsorbed CO_2, marked by the dashed ellipse and spindly oval, respectively. (e) and (f) Structural model of adsorbed CO_2 with vertical and inclined configurations. (g) Charge density difference of adsorbed CO_2. Differential electron density is integrated along the [001] direction. Red and blue isosurfaces represent electron gain and loss.

vacancy (BBO_V) sites, as the protrusions shown in Fig. 1(b). The apparent height of CO_2 is about 0.8 Å [see Figs. 1(c)–1(d)]. Here, CO_2 shows a different adsorption behavior comparing with CO, which preferentially adsorbs at Ti^{4+} site close to a BBO_V but not directly at the BBO_V.[22,23] By varying the CO_2 coverage, we found that CO_2 could appear at the Ti^{4+} sites only after all the BBO_Vs were completely filled by CO_2. With the excess exposure of CO_2, the diffusive CO_2 may occur at the Ti^{4+} site, but no stable adsorption configuration can be imaged, even at a much lower temperature of 15 K, as illustrated in Figs. 2(a)–2(d). Our observations are in agreement with the recent STM results.[24,25] They are also consistent with the temperature programmed desorption (TPD) results that the CO_2 binds to the BBO_V of Ti^{3+} sites more strongly than to fivefold-coordinated Ti^{4+} sites.[26–29] Sorescu *et al.*[24] calculated the adsorption configurations of CO_2 and compared with the STM images. They found that with the presence of BBO_V defect, the tilted configuration of CO_2 at the defect is the most stable one. Our density functional theory (DFT) calculations reveal both vertical and inclined configurations for the CO_2 linearly adsorbed at the BBO_V site, as schematically shown in Figs. 1(e)–1(f). The adsorption energy for the inclined configuration is lower by 0.16 eV than that for the vertical one. It seems like that the symmetric and asymmetric shapes of the adsorbed CO_2 in the occupied-state images could be attributed to these two configurations, as highlighted in the inset of Fig. 1(b). In other words, the coexistence of both adsorption configurations is highly possible. We have also calculated the charge transfer between the CO_2 and TiO_2 substrate and the results are given in Fig. 1(g). The net charge transfer between the CO_2 and TiO_2 substrate is small, however, the charge redistribution of CO_2 is obvious. To conclude, our experiments have shown that the CO_2 on the Ti^{4+} site at 80 K is not a stable configuration since it is very diffusive even at much lower temperatures [see Figs. 2(e)–2(g)]. The previously observed bright protrusions at the Ti^{4+} site at 80 K[24,25] could have resulted from species other than adsorbed CO_2 molecules.

We have conducted a series of STM experiments to examine the possible STM tip induced dissociation of CO_2. The obtained STM images show clear dissociation patterns, as given in Figs. 3(a)–3(c). It is found that the adsorbed CO_2 molecules at BBO_V can be removed when a relatively high voltage pulse is applied by the tip [see Figs. 3(b)–3(c)]. By comparing Fig. 3(c) with Fig. 3(a), it is clearly demonstrated that together with the disappearance of the CO_2 molecules, the original BBO_Vs also disappear. This strongly suggests that the CO_2 should be dissociated into an oxygen atom and a CO molecule, consistent with other experimental results.[25,30] At the Ti^{4+} sites shown at the lower-right of Fig. 3(c), the observed protrusions after the CO_2 dissociation are quite different from

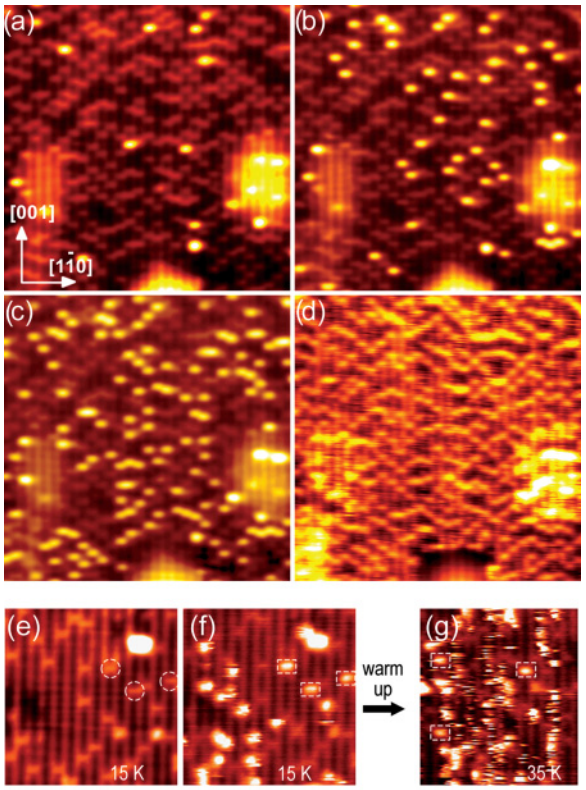

FIG. 2. (Color online) Consecutively acquired STM images during CO_2 dosing, (a) 0.2 Langmuir, (b) 0.8 Langmuir, (c) 1.5 Langmuir, and (d) 5 Langmuir. Size: 20.0×20.0 nm^2, imaging conditions: 1.4 V, 10 pA, at 80 K. (e) and (f) STM images of TiO_2(110)-1 × 1 surface before and after CO_2 adsorption within the same area, recorded at 15 K (size: 9.1×9.3 nm^2). (g) STM image of the CO_2 adsorbed sample recorded at 35 K (size: 9.1×10.2 nm^2). The image in (g) was taken from a different area due to the thermal drift during warm up of the sample. The adsorbed CO_2 molecules at BBO_Vs are immobile, but the CO_2 molecules at Ti^{4+} row are diffusive even at 15 K, and their diffusion becomes much faster at 35 K. Imaging conditions: 1.4 V, 5 pA.

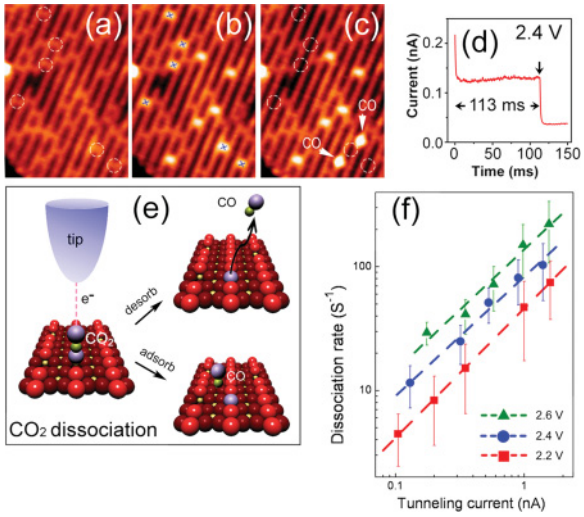

FIG. 3. (Color online) (a) Images of bare TiO_2(110)-1 × 1 surface, (b) after CO_2 adsorption *in situ* at 80 K, and (c) after tip-induced CO_2 dissociation (size: 8.5×11.9 nm^2, imaging conditions: 1.0 V, 10 pA.) (d) A typical I-t curve during the voltage pulse. (e) Schematic drawing of the tip-induced CO_2 dissociation, leading to the healing of the BBO_V and either desorbed CO or adsorbed CO at Ti^{4+} site. (f) Plot of CO_2 dissociation as a function of the tunneling current measured at different bias voltages.

that of the adsorbed CO_2, but fit well with the CO adsorption behavior as we observed before.[22] Such protrusions at the Ti^{4+} sites can be attributed to the readsorbed CO molecules, the dissociation product of the CO_2. Considering that the CO product from the tip-induced CO_2 dissociation can be trapped in the small space between the tip and the sample surface, we believe that the observed readsorption of about 20–30% CO is reasonable in our experiment. In general, as schematically shown in Fig. 3(e), after the dissociation, the oxygen atom occupies the BBO_V vacancy and the CO molecule either desorbs from the surface or adsorbs at Ti^{4+} site. One could imagine that it might not be practical if one uses TiO_2 to directly dissociate CO_2 into CO with such a one-step process, since the generation of the BBO_Vs requires extra actions on the TiO_2 surface, such as ion sputtering or annealing to a high temperature.

A typical current-time (I-t) curve is presented in Fig. 3(d), recorded during applying the voltage pulse. The current jump marked by the arrow in the I-t curve reflects the dissociation of CO_2, which could be used to measure its dissociation rate. The tip-induced dissociation rate as a function of tunneling current at different bias voltages is plotted in Fig. 3(f). The dependence on the current is linear with a slope of 0.98 ± 0.10 (2.6 V), 0.96 ± 0.07 (2.4 V), and 1.05 ± 0.01 (2.2 V) in the log-log plots, respectively. These values clearly imply that the dissociation process involves only one injected electron per dissociation event, ruling out the nonlinear "vibrational-heating" mechanism.[31,32] Such one-electron process could happen only if the tunneling electrons are directly injected into the lowest unoccupied molecular orbital (LUMO) of the adsorbed CO_2. It can thus be used to determine the reduction potential of the CO_2 upon adsorption. During revision of this manuscript, we noticed that a similar result was obtained by Lee *et al.*[30] with also a similar mechanism suggested.[30,33] Here, the presence of the BBO_V that possesses excess electrons plays an important role to complete the dissociation of CO_2 once $CO_2^{\bullet -}$ forms by injecting a tunneling electron. $CO_2^{\bullet -}$ dissociates into a neutral CO and an O^- ion, followed by the O^- ion heals the BBO_V, similar to the O_2 dissociation at BBO_V.[34,35]

Figures 4(a)–4(c) and 4(d)–4(f) show two sets of images during the CO_2 dissociation period at relatively high bias voltages of 2.0 and 2.6 V. It is found that when the surface is scanned with a bias voltage of 2.0 V, only a few of CO_2 can be dissociated, as marked by the arrow in Fig. 4(b). With a higher bias voltage of 2.6 V, nearly all of the CO_2 could be dissociated within the scanning area, accompanying with disappearance of the BBO_Vs and with occurrence of some CO at the Ti^{4+} sites, as shown in Figs. 4(d)–4(f). We have noticed that the diffusion of the adsorbed CO_2 at BBO_V is not observable even under relatively high bias voltages. The dissociation proportion as a function of the bias voltage is plotted in Fig. 4(g). It is noted that no dissociation event can be detected when the bias voltage is

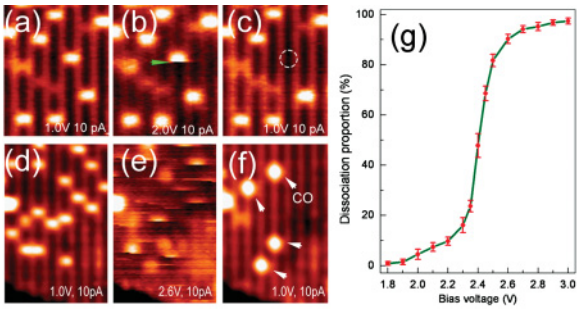

FIG. 4. (Color online) (a)–(c) A set of images showing CO_2 dissociation during scanning at 2.0 V (size: 3.9 × 4.7 nm^2). (d)–(f) Another set of images showing CO_2 dissociation during scanning at 2.6 V (size: 5.1 × 8.5 nm^2). (g) Dissociation proportion of adsorbed CO_2 at BBO_V as a function of the applied bias voltage.

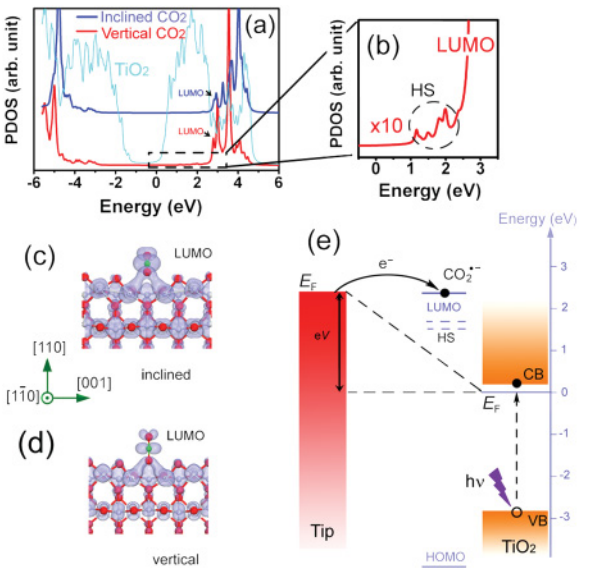

FIG. 5. (Color online) (a) PDOS of adsorbed CO_2 at BBO_V with vertical and inclined configurations, respectively. The PDOS is shifted from each other for clarity. (b) Magnified PDOS range showing weak hybridization states below LUMO. (c) and (d) Charge density distribution of LUMO in both of the vertical and inclined adsorption configurations, respectively. (e) Illustration of the formation of $CO_2^{\bullet-}$ excited state through tunneling electron attachment.

below 1.8 V, which could be regarded as the voltage threshold for the dissociation of the CO_2, consistent with the recently reported value of 1.7 V.[30] Moveover, a distinct increase of the dissociation proportion appears when the applied bias voltage is higher than 2.3 V. Such behavior is hardly dependent on the set point current in the range of 10 pA to 10 nA. It was known that the tip-sample distance varying from 9.0 to 4.5 Å resulted in the current changing from 10 pA to 10 nA at 1.6 V.[36] Here, the change of the tip-sample distance and the change of electric field have a very small effect on the CO_2 dissociation threshold and the dissociation proportion. As pointed out by Lee,[30] the electric-field-induced dissociation of CO_2 can be ruled out since the electric field in such experiment is much less than the minimum value of 40 V/nm required to dissociate a CO_2 molecule.[37] We also tried to dissociate the CO_2 using the negative bias voltages from −1.8 to −4.0 V, but did not observe any dissociation events. This means the dissociation of CO_2 can only happen by the electron injection. We also performed the experiment by illuminating the CO_2 adsorbed sample with UV light and pulsed laser of wavelength of 266 nm, with the method described elsewhere,[38] but failed to observe any CO_2 dissociation events, although some of the CO_2 may hop between BBO_Vs.

It should be mentioned that the tip-induced dissociation of molecules on solid surfaces using STM has been observed in other molecular systems.[31,32,34,35,39,40] Generally, such dissociation is attributed to the inelastic tunneling electrons (IETE) that induce vibrational excitations[31] or electronic excitation[41] of the adsorbed molecules. In this case, IETE services as an energy source and the total number of electrons in the molecule remains the same during the dissociation process. Our experimental results have strongly indicated that the CO_2 dissociation is most likely to be a one-step reduction process, in which a tunneling electron is attached to the CO_2 adsorbed on BBO_V to form $CO_2^{\bullet-}$. To confirm the hypothesis and understand our experimental results, we have carried out first-principles calculations to examine the interaction of the adsorbed CO_2 with TiO_2 surface and to determine the energy level alignment of CO_2 upon adsorption on TiO_2 that controls the electron attachment process.

Figure 5(a) gives the calculated partial density of states (PDOS) of the adsorbed CO_2 molecule at BBO_V. It is observed that the energy gap of the adsorbed CO_2 almost maintains that of the free CO_2 in both of the vertical and inclined adsorption configurations. It is well known that the DFT calculations give underestimated TiO_2 band gap.[42] However, it is reasonable to assume that the relative energy of the molecular orbitals with respect to the CB onset of TiO_2 could be well described by DFT. The I-V curves measured on TiO_2(110) surface show that the current onset at positive bias is about 0.4 V,[42] which indicates that the conduction band (CB) onset is nearly 0.4 eV above the Fermi level, consistent with the reported value of 0.3 eV.[43] The TiO_2 CB onset of our calculated PDOS is aligned according to the experimental result. The calculated CO_2 LUMO locates above the CB onset of TiO_2 by 2.3 eV, or 2.7 eV above the Fermi level for both of the vertical and the inclined adsorption configurations. It can be seen that the LUMO strongly hybridizes with the Ti 3d orbital of the BBO_V [see Figs. 5(c) and 5(d)]. From the energetic point of view, it is difficult to excite the electrons directly from the valence band (VB) to the LUMO of CO_2. Also, it is difficult for the excited electron to transfer from the CB of TiO_2 to CO_2 because of fast relaxation. This explains why the one-step reduction of CO_2 could not be observed under the photoexcitation.

As we discussed above, CO_2 can be dissociated through the electron attachment by injecting electron into the LUMO of the adsorbed CO_2. Although the calculated LUMO energy is not in perfect agreement with the experimental value, the theoretical results can still help to understand the underlying dissociation mechanism. As illustrated in Fig. 5(e), when the applied voltage makes the Fermi level of the tip match the LUMO of CO_2, the direct injection of the electron into the LUMO of CO_2 molecule becomes highly feasible, forming activation state of $CO_2^{\bullet-}$. It is found experimentally that at the voltage 2.3 eV, a rapid increase of the dissociation proportion takes place [see Fig. 4(g)], at which the best match is anticipated. In other

words, one can determine that the LUMO of CO_2 molecule should be located above the Fermi level by 2.3 eV, or above the TiO_2 CB onset by 1.9 eV. This value is much smaller than the estimated value of 3.5 eV by Indrakanti *et al*.,[3] and larger than the value of 1.6 eV (or −1.9 V versus SHE) in the aqueous solution.[19] The hybridized states from the interaction of CO_2 with the surface, as shown in Fig. 5(b), can spread over certain energy range, which is the major reason behind the observed threshold for the CO_2 dissociation.

IV. SUMMARY

In summary, we have studied the adsorption behavior of CO_2 molecules on TiO_2(110)-1 × 1 surface using *in situ* STM at 80 K. Our findings suggest that the CO_2 adsorbs on the top of BBO_V at low coverage and the CO_2 dissociation is induced by the attachment of the tunneling electron from the tip. Such a hypothesis is confirmed by first-principles calculations. With STM experiments, the exact location of the CO_2 LUMO that contributes to the formation of the CO_2 radical can be firmly determined, which helps to understand the preconditions for the photoexcitation process and to find ways to improve the efficiency for the conversion of CO_2 into CO and other carbonyl compounds, such as methanol synthesis and methane production.

ACKNOWLEDGMENTS

This work was supported by NBRP (Grants Nos. 2011CB921400 and 2010CB923300) and NSFC (Grants Nos. 9021013, 10825415, 10874164, and 21003113), China.

*bwang@ustc.edu.cn
†jghou@ustc.edu.cn

[1] R. Lal, Energy Environ. Sci. **1**, 86 (2008).
[2] C. S. Song, Catal. Today **115**, 2 (2006).
[3] V. P. Indrakanti, J. D. Kubicki, and H. H. Schobert, Energy Environ. Sci. **2**, 745 (2009).
[4] T. W. Woolerton *et al*., J. Am. Chem. Soc. **132**, 2132 (2010).
[5] S. C. Roy, O. K. Varghese, M. Paulose, and C. A. Grimes, Acs Nano **4**, 1259 (2010).
[6] M. Matsuoka, M. Kitano, M. Takeuchi, M. Anpo, and J. M. Thomas, Top. Catal. **35**, 305 (2005).
[7] M. Grätzel, Nature (London) **414**, 338 (2001).
[8] M. V. Ganduglia-Pirovano, A. Hofmann, and J. Sauer, Surf. Sci. Rep. **62**, 219 (2007).
[9] K. Koči, L. Obalová, L. Matějová, D. Plachá, Z. Lacný, J. Jirkovský, and O. Šolcová, Appl. Catal. B-Environ. **89**, 494 (2009).
[10] H. C. Yang, H. Y. Lin, Y. S. Chien, J. C. S. Wu, and H. H. Wu, Catal. Lett. **131**, 381 (2009).
[11] A. H. Yahaya, M. A. Gondal, and A. Hameed, Chem. Phys. Lett. **400**, 206 (2004).
[12] N. Sasirekha, S. J. S. Basha, and K. Shanthi, Appl. Catal. B-Environ. **62**, 169 (2006).
[13] E. E. Barton, D. M. Rampulla, and A. B. Bocarsly, J. Am. Chem. Soc. **130**, 6342 (2008).
[14] H. Arakawa *et al*., Chem. Rev. **101**, 953 (2001).
[15] T. Inoue, A. Fujishima, S. Konishi, and K. Honda, Nature (London) **277**, 637 (1979).
[16] J. Rasko and F. Solymosi, J. Phys. Chem. **98**, 7147 (1994).
[17] E. Fujita, Coordin. Chem. Rev. **186**, 373 (1999).
[18] H. J. Freund and M. W. Roberts, Surf. Sci. Rep. **25**, 225 (1996).
[19] W. H. Koppenol and J. D. Rush, J. Phys. Chem. **91**, 4429 (1987).
[20] G. Kresse and J. Hafner, Phys. Rev. B **47**, 558 (1993); **48**, 13115 (1993); **49**, 14251 (1994); G. Kresse and D. Joubert, *ibid*., **59**, 1758 (1999).
[21] P. J. D. Lindan, N. M. Harrison, M. J. Gillan, and J. A. White, Phys. Rev. B **55**, 15919 (1997).
[22] Y. Zhao, Z. Wang, X. F. Cui, T. Huang, B. Wang, Y. Luo, J. L. Yang, and J. G. Hou, J. Am. Chem. Soc. **131**, 7958 (2009).
[23] Z. Wang, Y. Zhao, X. F. Cui, S. J. Tan, A. D. Zhao, B. Wang, J. L. Yang, and J. G. Hou, J. Phys. Chem. C **114**, 18222 (2010).
[24] D. C. Sorescu, J. Lee, W. A. Al-Saidi, and K. D. Jordan, J. Chem. Phys. **134**, 104707 (2011).
[25] D. P. Acharya, I., N. Camillone, and P. Sutter, J. Phys. Chem. C **115**, 12095 (2011).
[26] M. A. Henderson, Surf. Sci. **400**, 203 (1998).
[27] T. L. Thompson, O. Diwald, and J. T. Yates, J. Phys. Chem. B **107**, 11700 (2003).
[28] S. Funk, B. Hokkanen, E. Johnson, and U. Burghaus, Chem. Phys. Lett. **422**, 461 (2006).
[29] G. B. Raupp and J. A. Dumesic, J. Phys. Chem. **89**, 5240 (1985).
[30] J. Lee, D. C. Sorescu, and X. Deng, J. Am. Chem. Soc. **133**, 10066 (2011).
[31] B. C. Stipe, M. A. Rezaei, W. Ho, S. Gao, M. Persson, and B. I. Lundqvist, Phys. Rev. Lett. **78**, 4410 (1997).
[32] S. Pan, Q. Fu, T. Huang, A. D. Zhao, B. Wang, Y. Luo, J. L. Yang, and J. G. Hou, Proc. Natl. Acad. Sci. USA **106**, 15259 (2009).
[33] L. G. Christophorou, D. L. McCorkle, and A. A. Christodoulides, in *Electron-Molecular Interactions and Their Applications*, edited by L. G. Christophorou (Academic, New York, 1983), Vol. 1.
[34] S. J. Tan, Y. F. Ji, Y. Zhao, A. D. Zhao, B. Wang, J. L. Yang, and J. G. Hou, J. Am. Chem. Soc. **133**, 2002 (2011).
[35] P. Scheiber, A. Riss, M. Schmid, P. Varga, and U. Diebold, Phys. Rev. Lett. **105**, 216101 (2010).
[36] X. F. Cui, Z. Wang, S. J. Tan, B. Wang, J. L. Yang, and J. G. Hou, J. Phys. Chem. C **113**, 13204 (2009).
[37] M. Calvaresi, R. V. Martinez, N. S. Losilla, J. Martinez, R. Garcia, and F. Zerbetto, J. Phys. Chem. Lett. **1**, 3256 (2010).
[38] C. Y. Zhou, Z. F. Ren, S. J. Tan, Z. B. Ma, X. C. Mao, D. X. Dai, H. J. Fan, X. M. Yang, J. LaRue, R. Cooper, A. M. Wodtke, Z. Wang, Z. Y. Li, B. Wang, J. L. Yang, and J. G. Hou, Chem. Sci. **1**, 575 (2010).
[39] O. Bikondoa, C. L. Pang, R. Ithnin, C. A. Muryn, H. Onishi, and G. Thornton, Nat. Mater. **5**, 189 (2006).
[40] B. C. Stipe, M. A. Rezaei, and W. Ho, Phys. Rev. Lett. **81**, 1263 (1998).
[41] H.-J. Shin, J. Jung, K. Motobayashi, S. Yanagisawa, Y. Morikawa, Y. Kim, and M. Kawai, Nat. Mater. **9**, 442 (2010).
[42] T. Minato, Y. Sainoo, Y. Kim, H. S. Kato, K. Aika, M. Kawai, J. Zhao, H. Petek, T. Huang, W. He, B. Wang, Z. Wang, Y. Zhao, J. L. Yang, and J. G. Hou, J. Chem. Phys. **130**, 124502 (2009).
[43] W. A. Tisdale, K. J. Williams, B. A. Timp, D. J. Norris, E. S. Aydil, and X.-Y. Zhu, Science **32**, 1543 (2010).